Eur. Phys. J. Plus (2022) 137:673
https://doi.org/10.1140/epjp/s13360-022-02876-4

THE EUROPEAN PHYSICAL JOURNAL PLUS

Regular Article

Particle detection in rare gas solid crystals: a feasibility experimental study—exploring new ways for dark matter searches

Exploring new ways for dark matter searches

Marco Guarise[a]

Dipartimento di Fisica e Scienze della Terra, Università di Ferrara and INFN Ferrara, Via Saragat 1, 44122 Ferrara, Italy

Received: 30 December 2021 / Accepted: 23 May 2022

Abstract This article reviews the experimental activity that has been carried out within the INFN DEMIURGOS research and development (R&D) project. This R&D concerns the study of possible innovative experimental approaches for the detection of low-energy-releases of feeble interacting particles within the matter. Possible applications could be the direct investigation of Dark Matter candidates. The idea behind the proposed scheme is to exploit rare gas solid crystals both pure and doped, combined with the in-vacuum single electron detection technology. In pure materials, the signal can be the charge produced directly during the ionization. Laser-assisted processes can instead be used to probe low-energy-releases in doped materials. Both these mechanisms should lead to a detectable electronic signal triggered by the incoming particle. In such a way, energy threshold ranging from meV to tens of eV could in principle be reached, opening-up the possibility to probe theoretically, well-motivated regions of unexplored electroweak parameter-space and thus test the existence of light Dark Matter candidates. The activity presented here has been performed to understand the mechanisms at the basis of the proposed detection scheme and possible showstopper. The experimental investigations refer to the research and development phases about: the crystal growing techniques and the corresponding set-up, the electrons' extraction from rare gas crystals to the vacuum environment, and finally the spectroscopic studies on atomic species embedded into rare gas matrices.

1 Introduction

Nowadays, one of the largest issue that we have to deal with is the problem of the "lacking mass" of the Universe. From observations on all cosmological and astrophysical scales, a remarkable result is in fact that there is something not visible but still contributing to the gravitational effect. From the historic point of view, this part of the Universe which is hidden has been called Dark Matter (DM) because it does not absorb or emit any electromagnetic radiation. It only interacts through the gravitational and, likely, the weak force. The first DM evidence [1] comes from the measure of the velocity dispersion of the galaxies in the Coma and Virgo clusters, which is too fast to form the cluster if one consider only luminous matter. Furthermore, numerous other indirect proofs of the Dark Matter existence were discovered and studied during the last 60 years. These are, for example, the rotational velocity of galaxies which does not decrease as expected $\propto r^{-1/2}$ outside the halo of visible matter [2], the gravitational lensing effect [3], the galaxy clustering observation, the Bullet cluster and finally the CMB anisotropies that can be used to infer the composition of the Universe [4].

Whatever the particles that compose the Dark Matter are, it is evident that they are characterized by a low interaction cross section with the ordinary matter which can be lower than the weak scale. Due to this fact, the detectors in this field have to deal with all the processes that happen at a low rate. Moreover, the background phenomenon must be almost absent in order to distinguish, with high statistical significance, true signals from the noise. This aspect, in particular, requires a diversification of all the complementary detectors that should be designed following different schemes and technologies offering the possibility to verify results in a detector-independent way [5].

Beyond this point, the second important aspect that we must consider is related to the various panoramas of possible constituents of Dark Matter. Theoretical proposals range from extremely light particles to the Massive Compact Halo Objects (MACHOs) that could be very heavy bodies of $\sim 10^{48}$GeV/c^2 [6]. In this scenario, one of the most favored candidates that has been searched through many direct experiments is the class of particles known as weakly interacting massive particles (WIMPs). These are non-baryonic Majorana particles without charge and color that represent a possible solution of the DM problem in a scenario of physics beyond the Standard Model (BSM) [7]. Experiments look for WIMPs mass in the GeV/c^2–TeV/c^2 range. Another possible candidate is the axion, a particle introduced by R. Peccei and H. Quinn in the 70s to solve the strong charge-conjugation-parity (CP) problem of

[a] e-mail: marco.guarise@fe.infn.it (corresponding author)

Published online: 08 June 2022

the Standard Model [8]. The axion mass can be expressed in terms of the symmetry breaking scale parameter [9] and this particle is expected to be very light (under the eV/c^2). Numerous and different particle detectors have been proposed, studied and built in order to search for candidates in this large scenario. Starting from the last decades, many detectors are taking data and are setting limits to the interaction cross section of DM particles.

Considering the state of the art, one of the most promising class of particle detector is the time projection chambers (TPC) based on the noble elements. As described in Sect. 2, noble elements present very interesting properties that can be exploited in this field. The best limit of $\sigma_{\mathrm{WIMP-Xe}} = 4.1 \times 10^{-47}\,\mathrm{cm}^2$ at $m_{\mathrm{WIMP}} = 30\,\mathrm{GeV/c}^2$ for WIMP nucleon cross section has been in fact reached through the XENON1T [10] detector that uses a large mass of liquid and gaseous xenon as active media. Other experiments that exploit this technology are for example PANDAX, LUX-LZ and DarkSide [11–16].

Given all these considerations, there is a huge effort of the scientific community to the research and the development of novel technologies for particle detectors in different fields such as novel active media, new detection approaches and innovative schemes in signal reading. This will lead to an improved generation of hybrid detectors with a high efficiency, a low background and a scalability potential, which are complementary to that of the current detectors. The experimental study shown here is part of this context and regards in particular the field of rare gas crystals solidified at cryogenic temperatures and the in-vacuum charge detection technology. The goal is in fact to reach high efficiency and low background solutions for particle detection [17,18].

Chemical and physical properties of the rare gases will be treated in Sect. 2.1, while rare gases crystals features will be described in Sect. 2.2. The proposed particle detection schemes are shown in Sect. 3. These ideas can be divided into two different areas, one concerns the undoped rare gas crystals described in Sect. 3.1, while the other regards the doped rare gas matrices described in Sect. 3.2. Finally, the fundamental experimental tests that have been carried out during the research and development phase of the project are shown in Sect. 4.

2 Rare gases

The rare gases (RG), also known as inert or noble gases, are the family of six elements belonging to the VIII group of the periodic table. Besides many applications in several fields, they have been used in the last four decades as active media for particle detectors thanks to a very exclusive combination of properties that make them interesting in the field of nuclear and particle physics [19].

2.1 Rare gas properties

The principal chemical and physical properties of the rare gases are shown in Table 1.

A key parameter related to the particle detection field is the ability of the RGs to stop and to absorb the incident radiation. When a quantity of energy is deposited into RG (liquid or solid), the processes that occur are the excitation, the ionization and the sub-excitation of the electrons. The parameters that describe and quantify such processes are the light yield and the ionization yield that represent the light and charge production per incident energy, respectively. Other important quantities are the drift velocity

Table 1 Properties of rare gases

Property	Ne	Ar	Kr	Xe
Atomic number Z	10	18	36	54
Melting temperature T_m (K)	24.56	83.81	115.78	161.40
Boiling temperature T_b (K)	27.10	87.30	119.93	165.05
Liquid density @ T_b ρ(g/cm^3)	1,21	1.39	2.42	2.94
Solid density @ T_m ρ(g/cm^3)	1.44	1.62	2.83	3.54
Refractive index in liquid at 0.5 μm R_i	1.23	1.23	1.30	1.38
Refractive index in solid at 0.5 μm R_i	–	1.23	1.35	1.44
Energy gap in liquid E_{gap} (eV)	–	13.4	11.55	11.67
Energy gap in solid E_{gap} (eV)	21.4	14.2	11.6	9.28
Electron mobility in liquid μ_e (cm^2/(Vs))	$1.6{\cdot}10^{-3}$[*]	475	1800	2950
Electron mobility in solid μ_e (cm^2/(Vs))	600	1000	3700	4500
MIP energy loss in liquid $\frac{\partial E}{\partial x}$ (MeV/cm)	2.04	2.105	3.28	3.7
Ionization yield in liquid CY (e$^-$/KeV)	–	7.4	–	4.7
Light Yield in liquid $\mathrm{LY_{liquid}}$ (γ/KeV)	7	40	25	46

"–" means that no value has been found in literature. *This value refers to the mobility of the "electron-bubble." The structure is composed of a macroscopic void that surrounds electron in liquid Neon. Data from Refs. [19–23]

Table 2 Fit parameters for Eq. 1 for several rare gases

Fit parameter	Ne	Ar	Kr	Xe
A	6.89224	7.66391	7.73270	7.78642
B	−110.809	−414.861	−578.32	−806.689
C	0.005434	0	0	0

Values from [25]

Table 3 Lattice parameter a of RG crystals

	Ne	Ar	Kr	Xe
a (Å)	4.43	5.26	5.72	6.20

and the V_0 energy which is the potential energy of the ground state of quasi-free electrons in the condensed media and represents how the electrons are favored to be emitted from the solid [24]. Finally, since we need to maintain the crystal into vacuum, the last parameter that we need to consider is the vapor pressure as a function of the temperature. The temperature trend of this parameter is as follows:

$$\log_{10} P = A + B/T + CT \tag{1}$$

where the pressure P is expressed in mbar, the temperature T in Kelvin and the values of the parameters for different RGs are shown in Table 2 [25].

2.2 Rare gas crystals

For the rare gases, crystallization occurs at cryogenic temperatures as shown in Table 1. These solids are considered molecular or atomic crystals since identical atoms bound by short range and weak van der Waals force occupies the crystal lattice sites. The modification of the long-range van der Waals due to the overlap of atomic excited states with the neighboring atoms in the crystal promotes the centrosymmetric cubic close pack (ccp) structure in RG [26]. The lattice parameter (a) for the main RG solid crystals is shown in Table 3.

Because of their low melting and sublimation points, special techniques and procedures are requested for the growth of RG crystals. Layers of RGs can be grown by a direct condensation of the gas onto a cooled substrate through the vapor deposition technique. Moreover, large samples whose dimensions can be greater than $\sim$100 cm^3 can be grown from the liquid phase in opportune containers following the so-called Bridgman–Stockbarger modified technique (BS). Both these techniques will be explained in the next paragraphs.

Vapor deposition technique This growing technique is the easiest way to form an RG solid. The solidification takes place when the gas is sprayed onto a cold surface at a temperature under the melting point, without the presence of the liquid phase. The uniformity of growing is ensured by an appropriate gas nozzle and the typical formation rate of 1 mm/h (or even lower) is guaranteed by the pressure of the gas inside the chamber, which is maintained in the 10^{-5} mbar range. This is a fact of particular importance since only with a low growing rate, it is possible to stack properly every layer of atoms and obtain thus high-optical-quality crystals. Following experimental observations, it is known that the maximum thickness of the crystal that can be obtained using this method is few millimeters.

It is also interesting to note that this technique is easily modifiable to obtain doped RG crystals. It is in fact sufficient to mix the rare gas with the doping atoms or molecules and then spray the mixtures to grow a doped crystal. In this method, named Matrix Isolation Technique (MIT) and initially proposed in the 50s by G. Pimentel [27], the guest particles (atoms, molecules or ions) are embedded within a continuous matrix of solid crystals (matrices) made of the inert gases. Following this technique, a very high density of guest particles can be obtained and, since the matrices are made of unreactive materials such as rare gases, only a feeble interaction between host and guest can take place [28].

Bridgman–Stockbarger modified method The principle at the basis of the BS technique is the slow solidification of the liquid phase [25]. This can happen in an appropriate container by translating the hot melt phase in the direction of growing, while a solid crystal is progressively formed behind the liquid. Initially, the chamber is filled with the liquid material at a temperature which is above the melting. Then, the temperature is slowly lowered at a certain rate, typically of the order of 1 Kelvin/hour, starting from the bottom part of the chamber. In such a way, a gradient of temperature is formed vertically along the direction of growing. Lowering the temperature, while maintaining a fixed gradient at $\sim 1-2$ K/cm necessary to grow uniformly, the portion of the container below the solidification temperature increases, and a large crystal is progressively formed. In order to obtain a structure with few defects, a uniform crystallization have to be obtained also in the horizontal plane. For such a reason, the radial dimension of the chamber cannot be too large. The technique above described is inspired to the Bridgman–Stockbarger method but is opportunely modified

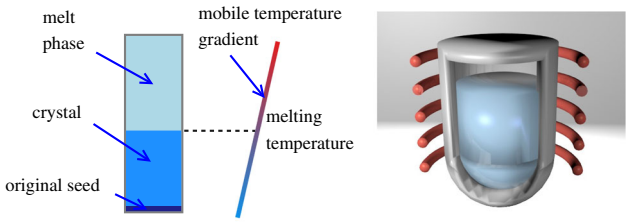

Fig. 1 Left side: sketch of the Bridgman–Stockbarger growing technique. Right side: drawing of a possible container surrounded by heaters (red rings)

to operate at cryogenic temperatures and it is also named liquid-freezing or gradient-freezing technique. Figure 1 shows a summary diagram of this technique and a sketch of a possible chamber for the BS growing technique.

3 Particle detection schemes in rare gases

As already said in Sect. 1, the proposed scheme for particle detector is based on rare gas crystals that can be used to probe light DM particles, such as WIMPs and axions, through two different schemes. The excellent properties of rare gas atoms, as described previously in Sect. 2, make these materials good candidates for hybrid detection schemes characterized by a low energy threshold, a high efficiency, a low background and that can be furthermore scaled-up to improve the active volume of the detector. The schemes have been conceived in the framework of an R&D project funded by the Italian Institute of Nuclear Physics (INFN) named DEMIURGOS. The first scheme exploits undoped rare gas crystals maintained at cryogenic temperature to detect heavy particles such as dark matter WIMPs. On the other side, the second scheme takes advantage of doped RG crystals. In this second case, the guests atoms, such as alkali metals or rare earth elements, can act as active centers where light particles such as axions can be absorbed. The detection occurs using laser-driven ionization techniques on the electronic energy levels of the guest atoms. In both the schemes, electrons detection can be performed through high-efficiency charge sensors characterized also by a very low background. The two schemes have many common elements, such as the matrices of rare gases and the development of many experimental processes is similar. In fact, the cooling system, the growing methods, the electrons' extraction and the electrons sensors are necessary for both the schemes. Furthermore, undoped RG crystals represent a first phase of the more complex doped scheme, which can be thought as an advanced phase.

3.1 Scheme in undoped crystals

The detection scheme proposed in undoped or pure crystals is based on the direct ionization of the rare gas atoms, when the incident particle, for instance DM, scatters with the target nucleus of RG. Electrons generated as a result of this process can drift within the RG crystal under an electric field and reach the crystal surface. Finally, they can be extracted and collected through suitable in-vacuum sensors characterized by a high sensitivity and a low background. Figure 2 shows a sketch of the detection scheme in such undoped crystals.

The process of electrons' extraction from the solid-vacuum interface can be described with a formalism that takes into account the potential energy V_0. The behavior of the electrons near the solid-vacuum interface can be described in terms of a 1-dim potential energy (V) with the coordinate z orthogonal to the surface plane and the origin in the surface [29]:

$$V(z) = \begin{cases} V_0 - eE_1 z + A_1 & z < 0 \\ -eE_2 z + A_2 & z > 0 \end{cases} \tag{2}$$

$$A_{1,2} = \frac{-e^2(\epsilon_1 - \epsilon_2)}{4\epsilon_{1,2}(z + \beta z/|z|)(\epsilon_1 + \epsilon_2)} \tag{3}$$

where E_1 and ϵ_1 are the electric field and the dielectric constant in the RG and E_2 and ϵ_2 are the electric field and the dielectric constant in vacuum. For continuity reason of the electric displacement field across the boundary, $\epsilon_1 E_1 = \epsilon_2 E_2$. β represents the thickness of the transition layer between the crystal and the vacuum. The electrons that have a momentum in the z-axis p_z, which is higher than the threshold value $p_0 \approx \sqrt{2m_e|V_0|}$, can be emitted through the solid-vacuum interface since they have sufficient energy. Depending on the sign of the potential barrier V_0, different pictures can happen. In the case of potential barrier negative and high in module ($|V_0| > K_b T$) such as in solid Krypton and Xenon, electrons in the solid must be accelerated by applying a strong electric field E in order to achieve an efficient emission. On the other hand, if V_0 is positive (in solid Neon and Argon), only a thin potential barrier has to be crossed by the electrons and the emission occurs efficiently at a very low electric field applied.

Thanks to the low temperature, the crystal is maintained in a vacuum environment ($P < 10^{-6}$ mbar) and when the electrons are released here, they can travel toward appropriate devices. Einzel lenses (ELs) or electrostatic mirrors could focus electrons into small spots where sensors with sufficiently high efficiency and low background rate are placed. Depending on the detection

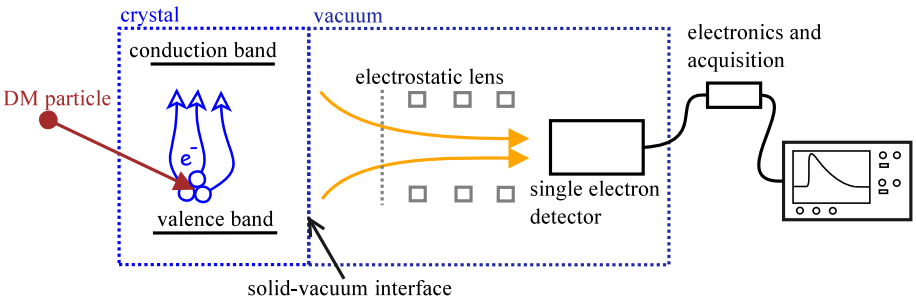

Fig. 2 Sketch of the proposed detection scheme in undoped crystals of rare gas. Ionization process occurs when the incoming particle hits the atom of the detector. Free electrons can drift within the crystal toward the solid–vacuum interface where they can be extracted in vacuum, and finally these electrons can be collected into suitable detectors

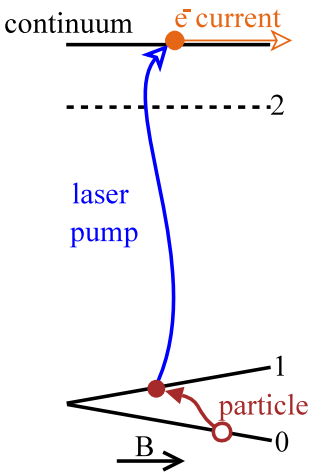

Fig. 3 Sketch of the laser upconversion scheme proposed in doped crystals. If the energy deposited by the interacting particle is resonant with a fixed value of the magnetic field B, the atom absorbs the energy. Starting from level 1, a tunable laser upconvert the state to the continuum providing the lacking energy to ionize the atom

scheme, three different kind of sensors have been considered: Multi-Channel Plate Assembly (MCPA), channeltron systems and fast luminescence phosphor coupled with light detectors. MCPA and channeltron are similar devices that works as electrons multipliers, are characterized by a single electron sensitivity and, depending on the dimensions, could have a dark count rate as low as $\sim$ 100 mHz [30].

3.2 Scheme in doped matrices

A low energy threshold scheme can be instead obtained in RG-doped crystals following a scheme similar to the InfraRed Quantum Counter (IRQC) concept proposed by the Nobel prize N. Bloembergen in the 50s to efficiently detect infrared (IR) photons [31].

In this case, looking for simplicity at the scheme shown in Fig. 3, the incident particle releases its low energy in the rare gas-doped crystal promoting the transition $0 \rightarrow 1$. Then, a laser pump (blue arrow in the figure) up-converts this level into the continuum, and the so-called laser-induced ionization takes place. This fact triggers the release of an electron into the rare gas matrix where it can drift under the electric field. Since this scheme is resonant to the transition $0 \rightarrow 1$, only the particles whose energy matches the energy difference between these two level (Δ_{01}) can be sensed [32,33]. To overcome this problem and increase the detection range, Δ_{01} can be opportunely tuned by exploiting the Zeeman effect using an external magnetic field B in the range $10^{-2} - 10$ T. The meaning of the tilted lines of levels 0 and 1 in the picture 3 is thus the possibility to tune the levels with B. In this scheme, the laser ionization efficiency can be easily expressed through the following equation:

$$\eta = \Phi_{ph}\sigma_1\tau_1 \tag{4}$$

where σ_1 is the ionization absorption cross section from level 1, τ_1 is the lifetime of the first level, and Φ_{ph} is the laser photons flux, which can be written as:

$$\Phi_{\text{ph}} = \frac{W_{\text{laser}}}{A_s \cdot h \cdot \nu} \tag{5}$$

where W_{laser} and ν are the laser power and photons frequency, respectively, h is the Planck constant and A_s is the area of the laser spot. Given the scheme, the linewidth of the transition $1 \rightarrow continuum$ plays an extremely important role, in fact this width must be smaller than the energy difference Δ_{01} to guarantee only the ionization of the atoms in the excited level. Any other laser absorption will in fact cause a spurious signal. To reduce this background noise, furthermore the transparency of the crystal at the laser pump wavelength is an important requirement. This can be obtained in high quality crystals where impurities and defects are almost absent.

4 Experimental tests

Rare gases at high level of purity have been used as starting material for all the tests to avoid the possible quenching of the signal, due to the charge trapping sites, that are mainly determined by high-electronegativity impurities such as oxygen [19]. The purification set-up used has been described in a paper already published [34], and guarantee a contamination of impurities lower than a part per billion (ppb). This part of the system is common for all the different set-up described in the following subsections.

Since RG solid crystals have never been used as particle detectors except in a few tests, the first investigation was to test the feasibility of growing pure and high-quality RG crystals. I decided to start the tests using a Neon crystal and grow it via the vapor deposition method, since this technique requires a set-up easier than the BS. The goals of this experimental test were to find a procedure for crystal growing that provides a sufficiently high crystal quality necessary for electrons' drift, and finally to demonstrate that electrons can be extracted from these solids into vacuum. The first measurements shown in Sect. 4.1 concerns the development of an apparatus for the growth of RG crystals using the vapor deposition method and a measure of the electrons' drift within the solid.

The second test that is described in Sect. 4.2 regards instead the scalability in large dimensions of the rare gas crystals. This test has been carried out exploiting the Bridgman–Stockbarger modified technique for the growth of a large Xenon crystal.

The last measurements, presented in Sect. 4.3 concern the study of doped crystals exploiting the matrix isolation technique. For simplicity reasons, only Neon and Argon have been used as matrices, and Rubidium, Samarium and Neodymium were exploited as dopants. In addition, since only few data regarding the physical behavior of these guest atoms in RG crystals have been found in literature, I decided to start the measurements from the basis and investigate these materials through optical spectroscopy both in emission and in absorption. As described previously, it is worth noting that the two important requirements necessary for the proposed detection scheme are the narrow width of the lines and their long lifetime.

4.1 Electrons extraction from solid Neon

As already said, the feasibility of growing pure and high-quality RG crystals is the primary experimental question. This point has been tested exploiting a Neon crystal, grown through the vapor deposition technique.

A picture of the apparatus is shown in Fig. 4 on the left side. The chamber consists of a four-hole cross stainless steel chamber equipped with four DN200 ConFlat flanges. The flange on the top hosts a two-stage-helium pulse tube refrigerator[1] that allows a minimum temperature of 4.2 K. The cold finger of the refrigerator is placed at the center of the chamber. The hole in the front side hosts instead the vacuum manipulator where the gas nozzle and the charge receiver disk (CRD) are mounted. Thanks to the manipulator, it is possible to set the one or the other in front of the cold finger. More details of this setup has been described in a previous paper [34].

A picture of the cold finger with the growth plate (GP) attached is shown in Fig. 4b). In the center of the GP, there is a 8-mm-diameter hole which is covered with a 100-nm-thickness gold foil evaporated on a substrate of 2-mm-thick UV grade fused silica window. This allows UV photons delivered by a frequency-quadrupled Q-switched Nd:YAG laser, to impinge on the gold surface. Photons bunches reach the GP in the vacuum chamber thanks to a 3-m-long quartz optical fiber. When 266-nm photons impinge on the gold, electrons are generated in the GP thanks to the photoelectric effect. These electrons can drift in the crystal, reach the solid-vacuum interface, and they can be extracted in vacuum where they are collected in the CRD.

The charge collected as a function of the electric field for the 1-mm-thick Neon crystal kept at 9 K is shown in Fig. 5. The charge signal is triggered after the laser pulse. The error bars come from statistical analysis. For an electric field applied between GP and CRD greater than 100 V/cm, full charge collection is accomplished. Starting from this value, the collected charge reaches in fact a plateau.

It is worth noting that the measured signals are real charges that impinge on the CRD and not spurious signals due as instance to laser pulses. For an absent electric field applied between GP and CRD, a null charge is in fact collected. Vice versa, if these signals were due to light, they would not present the electric field dependence which is instead shown in Fig. 5.

Moreover, the crystal growing procedure allows to obtain a solid crystal of Neon with a volume of about 0.5 cm^3 and a good optical quality that has also been found after a visual inspection. The signals measured at the CRD allow to do an important consideration regarding the crystal quality since the amplitude of the signal does not change during several hours of photo-injections in the crystal. Such an experimental observation means that electrons can drift in the same condition of electric field and thus no space-charge

[1] Sumitomo Corp. RP82B2.

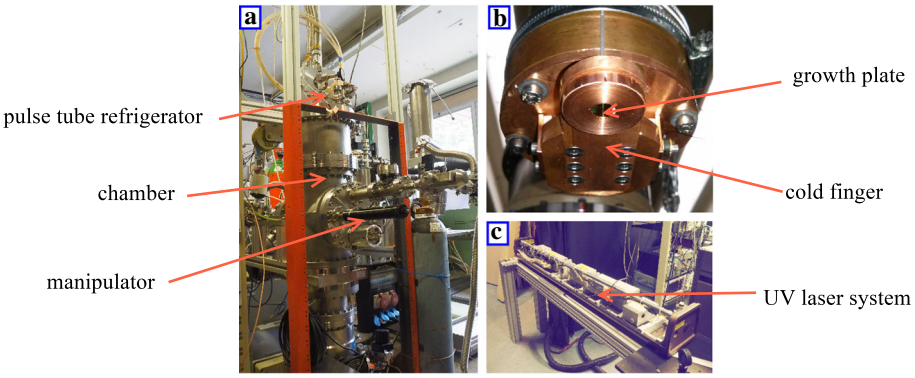

Fig. 4 Picture **a** is the photo of the cryostat chamber (front part). On the top of this picture we can see the pulse tube refrigerator and the optical fiber feedthrough. Picture **b** shows the copper growth plate. In the center, we can recognize the gold surface on the fused silica substrate. Finally, picture **c** shows the laser system

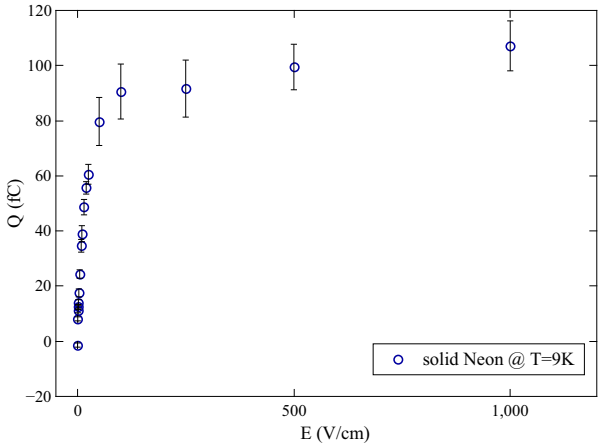

Fig. 5 Charge extracted from the solid Neon crystal and collected at the CRD as a function of the electric field

effect takes place in the Neon crystal. This ensures a good quality of the structure and a high purity level since impurities and imperfections in the lattice would act as charge attractors immediately after the crystal formation [19]. Reasonably, several hours of measurements can thus be considered a good compromise to test crystal quality at this level.

4.2 Large Xenon crystal

As described in Sect. 2.2, large samples of rare gas crystals can be grown through the Bridgman–Stockbarger modified technique. Following this procedure, an opportune apparatus composed of a 0.5 l Pyrex chamber, a cryogenic LN2 vessel and a feedback temperature controller has been built in order to grow a large Xenon crystal.

The growth chamber is inserted into a large liquid nitrogen (LN2) vessel and can be placed at a distance of 4 cm above the LN2 level. In this position, it is surrounded by the cryogenic nitrogen vapor, and the chamber's walls can reach a temperature down to ∼90 K. The growth chamber is a custom-made Pyrex container where the welding between the glass and the stainless-steel flange is made of Kovar, a metallic alloy that ensures an optimum contact between the parts without outgassing. Furthermore, this material has a thermal expansion coefficient very close to the one of Pyrex and makes thus possible the cooling of the chamber without cracks. The Pyrex chamber is a cylindrical container whose internal diameter is 63 mm and total length 120 mm. The chamber is connected to the gas purification system outside the LN2 vessel through a 1.5-m-long tube necessary to fill the container with Xenon (Fig. 6).

Inside the Pyrex chamber, three ceramic (Macor) supports hold the electrodes used for the measurement of the electrons drift inside Xenon crystal. The cathode consists of a 25-mm-diameter disk mounted 18 mm distant from the base of the chamber. Placed ∼18 mm above, there is the anode plate which is a 25-mm-diameter disk. A 21-mm-inner-diameter guard-ring is placed between them and ensures the homogeneity of the electric field. Finally, also a 97% transmittance copper grid is placed 3 mm away from the anode. The active volume included between the electrodes that delimit the drift region is ∼21 cm^3, while the total available volume inside the Pyrex chamber is about 150 cm^3. To guarantee an electric field of ∼ 500 V/cm in the drift region, the voltage of the electrodes has been set to – 1500 V, – 1000 V, – 520 V and ground for the cathode, guard-ring, grid and anode, respectively.

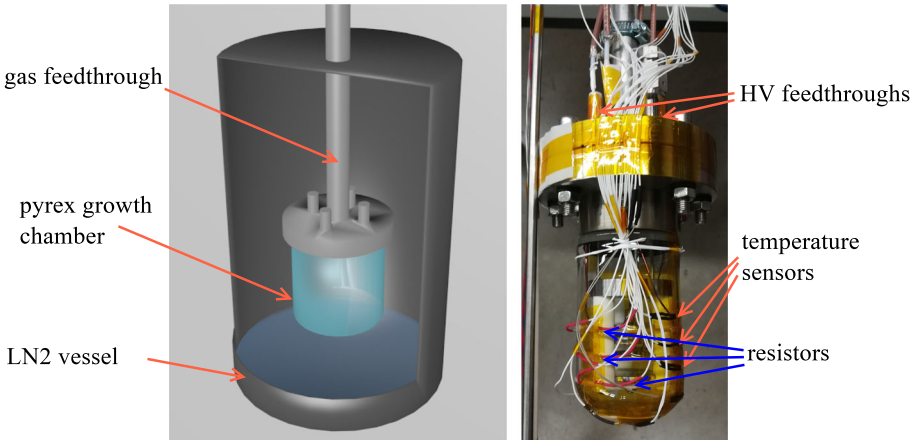

Fig. 6 Left: sketch of the setup used for the Bridgman–Stockbarger modified technique. Right: picture of the Pyrex chamber used for the growth of large Xenon. In the inner part of the Pyrex chamber are visible the 3 Macorholders (white columns) for the electrodes

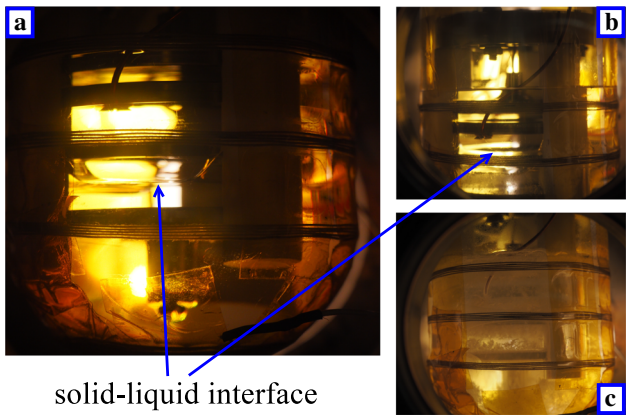

Fig. 7 Pictures taken during different attempts of crystal growing. The first **a** represents a good crystal, while in **b** defects start to form and finally in **c** a completely opaque structure has been obtained

Given the thermal conductivity of the Pyrex at 150 K, which is $\sim 1\,\mathrm{Wm^{-1}K^{-1}}$, the temperature T along the vertical direction of the chamber has been fixed every 1 cm through wire resistors with $R_{\mathrm{wire}} \sim 1\,\Omega$ glued at the Pyrex external walls. Furthermore, several platinum-resistive temperature sensors PT100 are placed near each wire and measure the local temperature T_{act}. An electronic module and a custom Labview program monitor the temperature of each point and set the current that flows in every resistive wire in order to obtain the desired temperature and temperature gradient along the chamber direction through a feedback system.

A slow growth has been operated to obtain a transparent solid with a good optical quality [35,36]. Once the chamber was filled with ~ 500 g of liquid Xenon at 163 K, a temperature gradient $\Delta T = 1$ K/cm was applied in the vertical direction starting from the bottom of the container, placed at 161 K. At this point, the temperature gradient has been progressively translated causing the progressive enhancement of the crystal structure. To guarantee a crystal formation uniform in the center and in the sides, the optimal velocity for crystal growing of $\simeq 1$ K/h has been set. The thickness of the solid (L) that can be obtained through this method can be estimated as [36]:

$$L = \sqrt{\frac{2K\Delta T}{H\rho}}\sqrt{t} \tag{6}$$

where $K = 0.001$ W/(cm.K) is the thermal conductivity of solid Xenon, ΔT is the temperature difference, H is the latent heat of fusion (17.5 J/g for Xe) and ρ is the density. Finally, t is the elapsed time since the formation began. This process ends when the liquid phase is no more available in the chamber.

Any modification of the recipe described above, for example a change in the temperature gradient or in the translation velocity, produces different kind of optical imperfections, such as white structures or opaque stains that appears as macroscopic volumes with a large number of voids and other kinds of defects. Furthermore, also mechanical movements and vibrations of the chamber can create faults in the crystal structure.

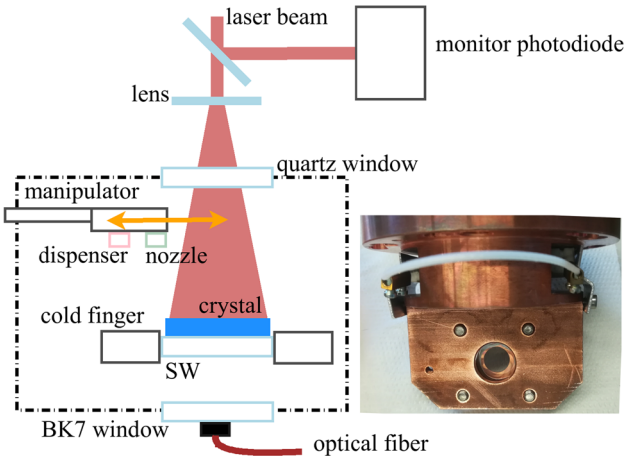

Fig. 8 Sketch of the experimental setup used for the vapor deposition growing technique. It is also shown the last part of the optical setup used for the excitation of the crystals. The inset picture shows the front part of the cold finger, where the sapphire window that can sustain the crystal is placed

Figure 7 shows three pictures taken during different crystal growth attempts. Picture (a) shows the crystal formation during a good test. Here, a completely transparent crystal is present in the bottom part of the chamber, while the liquid phase appears in the top part. The other two pictures (b) and (c) show crystals with imperfections as a consequence of a too rapid temperature decrease in the Pyrex chamber (∼5 K/30 min) due to a wrong cooling procedure. In particular, picture (c) shows a crystal with a large amount of defects that have completely destroyed the structure.

In order to check the crystal quality and furthermore test the operation of the crystal as a detector, the interaction of cosmic rays in the active part of solid Xenon included between anode and cathode, have been measured. A coincidence measure has been carried out through a scintillator coupled with a photomultiplier tube placed beyond the chamber. Free electrons (e^-) are formed when comic muons cross the crystal and release their energy ionizing the Xe atoms. Thanks to the electric field applied in the active region, these e^- can drift in the crystal and can be collected in the anode. The measurement of the charge acquired is then used to infer the energy deposited and thus reconstruct the spectrum that follows the usual Landau distribution [18]. The peak has been founded at (6.3±0.2) MeV which is in good agreement with the expected value of $\partial E/\partial x \cdot l \simeq 6.5$ MeV.

4.3 Doped matrices

In this section, the investigation through optical spectroscopy of doped crystals grown through the matrix isolation technique will be briefly described. As previously mentioned, only Neon and Argon were used as matrices, while Rubidium, Samarium and Neodymium were exploited as dopants. The first important thing to understand is in fact the behavior of guests and hosts atoms in rare gas doped crystals. Furthermore, in the view of particle detection, the two basic requirements are the narrow linewidths of the dopant atomic levels and their long lifetime.

For these tests, a specific apparatus that combines both the cryogenic and the optical part has been developed. A cross section sketch of the setup is shown in Fig. 8. The main block of the setup is a six-hole cross stainless steel chamber (SSC) that holds the pulse tube refrigerator (PTR).[2] The cold finger, that is placed in the center of the SSC, hosts a 25-mm-diameter sapphire window (SW) that can hold the crystal and allows optical transmission tests. Sapphire has a very broad optical transmittance from ∼ 200 nm to ∼ 5 μm that allows wide band spectroscopy. Moreover, sapphire has a good thermal conductivity also at cryogenic temperatures (at 10 K is ∼ 700 $Wm^{-1}K^{-1}$) which is necessary for RG crystals growing. A picture of the cold finger with the sapphire window mounted at its center is shown in the inset of Fig. 8. In the SSC, a quartz and a BK7 windows are mounted in the optical axis that passes through the SW, while in the transverse direction the SSC is equipped with a vacuum manipulator that hosts both the RG gas nozzle and the dopants dispenser. The manipulator allows to place these parts in front of the SW or 10 cm backward in order to perform optical transmission measurements. The precise temperature of the cold finger can be set using a 15 W resistive heater placed nearby the SW, exploiting the Joule effect. The temperature is measured with a Silicon diode temperature sensor.

The optical part of the setup consists of different lasers systems which are tunable in the visible (VIS) and in the near-infrared (NIR) ranges that are focused in the SW. In particular, we used CW-single-mode dye and titanium–sapphire (Ti:Sa) lasers with a typical linewidth of ∼GHz, pumped by a diode-pump-solid-state (DPSS) laser at 532 nm. Their output power ranges between 150 mW to 1 W, depending on the wavelength. The light detection system is based on different kinds of photodiodes and spectrometers in the

[2] Sumitomo Corp. RP82B2.

Table 4 Peak parameters for the excitation and emission lines as shown in Fig. 9

Peak	A (a.u.)	λ_c (nm)	W (nm)
Excitation	9900 ± 100	764.5 ± 0.1	7.2 ± 0.9
Emission	$15{,}700 \pm 800$	1270.1 ± 0.1	15.7 ± 0.2

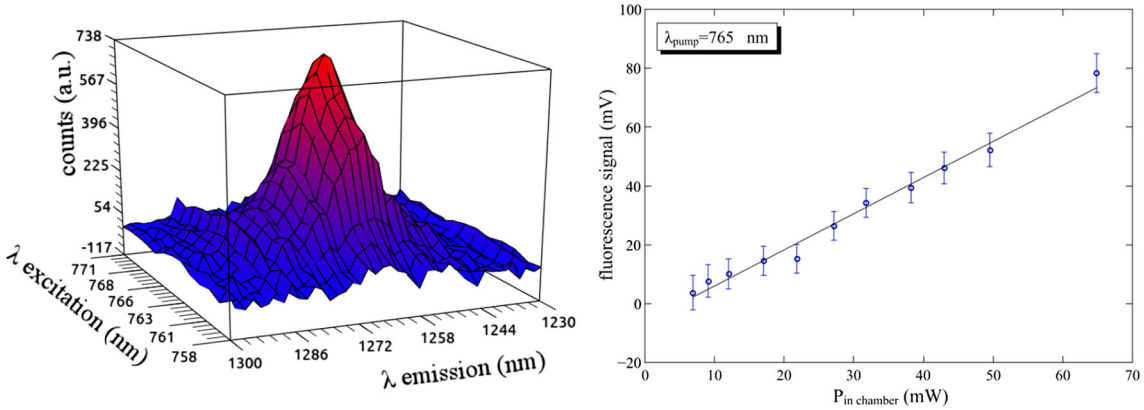

Fig. 9 Left: excitation-emission 3-dim plot of s-Ne:Rb. Right: fluorescence intensity as a function of the power incident in the chamber

UV,[3] VIS[4] and NIR[5] ranges. The measurements have been carried out in a completely dark environment to minimize the background noise.

The crystal growth happens by spraying the purified gas mixed with the doped materials onto the cold surface of the SW. The gas is sprayed through an opportune nozzle, while the dopant atoms evaporate from the dispenser whose temperature is controlled through the current that flows in it. The growing can be monitored by the following parameters: the partial pressure of the gas (P_g^{gas}) and the dopant (P_g^{dop}), the temperature (T_g) and the growing time (t_g). The first step in the growing is the formation of a $\sim$100 μm-thickness layer of pure rare gas, which forms the basis of the crystal. Then, the dispenser is activated and a formation of a doped crystal begins. During this phase, $P_g^{\text{gas}} \sim 5 \times 10^{-5}$ mbar, while $P_g^{\text{dop}} \sim 5 \times 10^{-7}$ mbar resulting in a doping of a small percentage [37]. The final step is to deposit the last 100 μm of pure RG above the doped matrix.

As an example, I have reported here some of the measurements carried out in a Neon crystal doped with rubidium (s-Ne:Rb) whose thickness is $\sim$1.5 mm. The highest emission intensity at $\lambda_{\text{emission}} \sim 1270$ nm was measured in an isolated peak when the crystal was pumped at $\lambda_{\text{excitation}} \sim 765$ nm. The peak shape is shown in the three-dimensional plot of Fig. 9 on the left. A Lorentzian fit was done independently for both excitation and emission using the function 7:

$$L(\lambda) = y_0 + 2 \cdot \frac{A}{\pi} \frac{W}{4(\lambda - \lambda_c)^2 + W^2} \tag{7}$$

where the free parameters of the curve are the area A, the width W and the central wavelength λ_c. Furthermore, an offset y_0 allows to correct for continuous light components. The results are listed in Table 4:

Finally, the linearity of the fluorescence intensity in the band 1.24–1.3 μm was measured as a function of the laser power at a fixed wavelength of 765 nm, as shown in Fig. 9 on the right. A good linearity was found in the investigated range.

5 Discussions and conclusions

The purpose of these experimental works was to study the feasibility and the possible applicability of novel particle detection schemes based on rare gas crystals. These innovative approaches have been proposed as a new and complementary class of hybrid detectors characterized by a low-energy threshold and a low background, required for the studies of feeble interaction and $\sim$eV-energy-release events. Many physical questions are, in fact, nowadays present and, from the experimental point of view, they could be addressed exploiting innovative detection schemes. In particular, one of these challenging issues is the lacking mass of the Universe, the Dark Matter. Many candidates, whose masses range from sub-eV to TeV, have been proposed in the last decades to solve this issue, and many experimental works are currently ongoing in this field. The last generation of detectors employed in DM

[3] Ocean Optics 200–850 nm.

[4] Ocean Optics 350–1050 nm and Thorlabs 550–1050 nm.

[5] Ocean Optics 950–1700 nm.

experiments are taking data nowadays, but unfortunately no direct experimental evidences of DM existence have been found yet. For this reason, it is important to improve the performances of the current detectors, looking for new sensors. In the framework of the INFN project DEMIURGOS, two different schemes that exploit rare gas crystals, both pure and doped, combined with the in-vacuum single electron detection technology, have been investigated. These hybrid concepts could open the possibility to investigate DM candidates which can hardly be probed otherwise. The experimental R&D phase that has been carried out until now regards the study of RG solids growing techniques, of electrons extraction from solid RG crystals, of large solids growing and of doped matrices formation. All these phenomena are fundamental in the detection approaches that has been proposed. These measurements are presented and described in this paper and play a crucial role for the development of particle detectors based on solid RG with a low-energy threshold and a low-background. In this R&D phase, no showstopper regarding the physical mechanisms involved in the detection schemes has been found. The major difficulty in the experimental part of the project occurred in the growth of very large RG crystals. This is probably due to the very low thermal conductivity and the large density variation in temperature of the solid RG. To overcome this issue, a possible solution can be to grow several smaller samples of RG solids instead of a unique large crystal. Moreover, other studies, especially regarding the low-energy detection idea in doped crystals, are necessary because of the lack of knowledge of many processes involved in such environments. A better understanding of these systems, which is important to compute and simulate their behavior as particle detector, requires in fact a deeper comprehension of some fundamental parameters, such as the interaction potential between host–host and host–guest and the ionization potential of dopant atoms in RG matrices. These features are in fact at the basis of the proposed scheme and must be known precisely before the application of doped matrices as particle detectors. Finally, the temperature dependence of charge transport properties in RG, the optical properties of RG matrices at low temperature and the effects of crystal defects and imperfection on electrical, mechanical and optical features of RG solids are other characteristics that should be investigated in more detail.

One of the main question regards the active volume that can be obtained. Large kg-scale pure crystals of RG can be easily obtained and thus in the view of a large-scale experiment, many crystals can be coupled to form a single detector, such as other experiments designed for the detection of rare events [38,39]. Doped crystals can instead be grown in the form of long cylinders with a radius of few mm. In such a way, the laser probe needed to detect the incident particle can match the crystal volume. In any case, a good doped crystal with a volume of liter can be difficultly attained using the techniques exploited so far and described in this paper. The sensitivity of the proposed schemes is another important characteristic which must be considered. This parameter is strictly related both to the electrons' detector efficiency and to the crystal features. In particular, the limiting factor for the sensitivity is represented by the background noise. In the final detector, background signals are one of the major drawback and should be avoided or discriminated as much as possible. The dark count rate of electrons' detectors, which could be lower than 0.01 Hz/mm^2 for a single electron event, could be discriminated using a threshold at few electrons. On the other hand, cosmic rays interactions in the detector represent the largest source of false signals, and they can only be diminished by placing the detector in underground laboratories where cosmic rays flux is smaller. As in other DM detectors, also muons veto systems can be installed in the proximity of the detector, allowing the identification of muon interaction events. Another source of background can be related to the presence of radioactive isotopes, such as Potassium 40, which decays β or γ releasing 1.3 MeV or 1.5 MeV, respectively. Usually, these events cannot be avoided and an inner volume, where the noise suppression is at a high level, can be identified. This region is commonly named fiduciary volume with zero background and represents the active region of the detector. Regarding the approach in doped matrices, a possible source of background noise can be the laser pump. In suitable materials, however, non-resonant absorption can be neglected and the laser absorption is triggered only when the transition between ground state and first excited levels occurs. The validity of this behavior has been demonstrated in the so-called laser cooling of solids [40,41], where, in proper conditions, tens of W/cm^2 of photons impinge on a crystal and a cooling to cryogenic temperatures happens. Moreover, due to the narrow linewidth of axions, the signal induced by these particle is resonant with a precise value of the energy difference, and it could be identified from the white noise background as a sharp peak at a certain energy.

Finally, I would like to remark that the studies that have been carried out regarding RG crystals used as particle detectors, can be very useful also in other fields of researches. In particular, the study of the behavior of the rare gases in their solid phase can have applications in medicine, industry and fundamental physics studies.

Acknowledgements This paper reviews the work that has been carried out during my Phd period. The work was awarded by INFN through the prize F. Resmini for the best Phd research activity in the field of accelerator physics and new technology. I would like to thank C. Braggio, R. Calabrese, G. Carugno and L. Tomassetti for the enormous support and the helpful discussions. Moreover, all the experimental activities have been possible thanks to the technical support of E. Berto, F. Calaon and M. Tessaro.

Funding Open access funding provided by Università di Ferrara and INFN Ferrara within the CRUI-CARE Agreement.

Data Availability Statement This manuscript has associated data in a data repository. [Authors' comment: The datasets analyzed during the current study are available from the corresponding author on reasonable request.]

Declarations

Conflict of interest The author declares that he have no known competing financial interests or personal relationships that could have appeared to influence the work reported in this paper.

References

1. F. Zwicky, Die rotverschiebung von extragalaktischen nebeln. Helv. Phys. Acta **6**, 110–127 (1933)
2. K.G. Begeman, A.H. Broeils, R.H. Sanders, Extended rotation curves of spiral galaxies: dark haloes and modified dynamics. Mon. Not. R. Astron. Soc. **249**(3), 523–537 (1991)
3. D. Walsh, R.F. Carswell, R.J. Weymann, 0957+ 561 a, b: twin quasistellar objects or gravitational lens? Nature **279**(5712), 381 (1979)
4. N. Aghanim, Y. Akrami, M. Ashdown, J. Aumont, C. Baccigalupi, M. Ballardini, A.J. Banday, R.B. Barreiro, N. Bartolo, S. Basak, et al. Planck 2018 results. vi. cosmological parameters. arXiv:1807.06209 (2018)
5. M. Battaglieri, A. Belloni, A. Chou, P. Cushman, B. Echenard, J. Essig, R. Estrada, J.L. Feng, B. Flaugher, P.J. Fox, et al. Us cosmic visions: new ideas in dark matter 2017: community report. arXiv:1707.04591 (2017)
6. A.V. Zasov, A.S. Saburova, A.V. Khoperskov, S.A. Khoperskov, Dark matter in galaxies. Phys. Usp. **60**(1), 3 (2017)
7. M. Pospelov, A. Ritz, M. Voloshin, Secluded wimp dark matter. Phys. Lett. B **662**(1), 53–61 (2008)
8. R.D. Peccei, The strong cp problem and axions, in *Axions* (Springer, 2008), pp. 3–17
9. V.B. Klaer, G.D. Moore, The dark-matter axion mass. arXiv:1708.07521 (2017)
10. X.E.N.O.N. Collaboration, E. Aprile, J. Aalbers, F. Agostini, M. Alfonsi, L. Althueser, F.D. Amaro, M. Anthony, F. Arneodo, L. Baudis et al., Dark matter search results from a one ton-year exposure of xenon1t. Phys. Rev. Lett. **121**(11), 111302 (2018)
11. D.S. Akerib, S. Alsum, H.M. Araujo, X. Bai, J. Balajthy, P. Beltrame, E.P. Bernard, A. Bernstein, T.P. Biesiadzinski, E.M. Boulton et al., Search for annual and diurnal rate modulations in the lux experiment. Phys. Rev. D **98**(6), 062005 (2018)
12. H. Zhang, A. Abdukerim, W. Chen, X. Chen, Y. Chen, X. Cui, B. Dong, D. Fang, C. Fu, K. Giboni et al., Dark matter direct search sensitivity of the pandax-4t experiment. Sci. China Phys. Mech. Astron. **62**(3), 31011 (2019)
13. P. Agnes, T. Alexander, A. Alton, K. Arisaka, H.O. Back, B. Baldin, K. Biery, G. Bonfini, M. Bossa, A. Brigatti et al., First results from the darkside-50 dark matter experiment at laboratori nazionali del gran sasso. Phys. Lett. B **743**, 456–466 (2015)
14. J. Howlett, E. Aprile, The xenonnt dark matter search experiment. Bull. Am. Phys. Soc. **64**, H17-006 (2019)
15. D.S. Akerib, C.W. Akerlof, S.K. Alsum, H.M. Araujo, M. Arthurs, X. Bai, A.J. Bailey, J. Balajthy, S. Balashov, D. Bauer, et al., Projected wimp sensitivity of the lux-zeplin (lz) dark matter experiment. arXiv:1802.06039 (2018)
16. J. Aalbers, F. Agostini, M. Alfonsi, F.D. Amaro, C. Amsler, E. Aprile, L. Arazi, F. Arneodo, P. Barrow, L. Baudis et al., Darwin: towards the ultimate dark matter detector. J. Cosmol. Astropart. Phys. **2016**(11), 017 (2016)
17. M. Guarise, C. Braggio, R. Calabrese, G. Carugno, A. Dainelli, A. Khanbekyan, E. Luppi, E. Mariotti, L. Tomassetti, Particle detection in rare gas solids: demiurgos experiment. Nucl. Instrum. Methods Phys. Res. Sect. A **958**, 162434 (2020)
18. M. Guarise, C. Braggio, R. Calabrese, G. Carugno, A. Dainelli, A. Khanbekyan, E. Luppi, E. Mariotti, L. Tomassetti, A feasibility study for a low energy threshold particle detector in a xenon crystal. J. Instrum. **15**(03), C03004 (2020)
19. E. Aprile, A.E. Bolotnikov, A.I. Bolozdynya, T. Doke, *Noble Gas Detectors* (Wiley, New York, 2006)
20. A.C. Sinnock, B.L. Smith, Refractive indices of the condensed inert gases. Phys. Rev. **181**, 1297–1307 (1969)
21. P. Sorensen, A. Manzur, C.E. Dahl, J. Angle, E. Aprile, F. Arneodo, L. Baudis, A. Bernstein, A. Bolozdynya, L.C.C. Coelho et al., The scintillation and ionization yield of liquid xenon for nuclear recoils. Nucl. Instrum. Methods Phys. Res. Sect. A **601**(3), 339–346 (2009)
22. A. Bondar, A. Buzulutskov, A. Dolgov, E. Grishnyaev, V. Nosov, V. Oleynikov, S. Polosatkin, L. Shekhtman, E. Shemyakina, A. Sokolov, Measurement of the ionization yield of nuclear recoils in liquid argon using a two-phase detector with electroluminescence gap. J. Instrum. **12**(05), C05010 (2017)
23. W.M. Haynes, *CRC Handbook of Chemistry and Physics* (CRC Press, London, 2014)
24. W. Schmidt, *Liquid State Electronics of Insulating Liquids* (CRC Press, London, 1997)
25. M.L. Klein, J.A. Venables, *Rare Gas Solids*, vol. 1 (Academic Press, London, 1976)
26. K.F. Niebel, J.A. Venables, An explanation of the crystal structure of the rare gas solids. Proc. R. Soc. Lond. A. Math. Phys. Sci. **336**(1606), 365–377 (1974)
27. E. Whittle, D.A. Dows, G.C. Pimentel, Matrix isolation method for the experimental study of unstable species. J. Chem. Phys. **22**(11), 1943–1943 (1954)
28. I.R. Dunkin, *Matrix-Isolation Techniques: A Practical Approach* (Oxford University Press, Oxford, 1998)
29. A.I. Bolozdynya, Two-phase emission detectors: foundations and applications. IEEE Trans. Dielectr. Electr. Insul. **13**(3), 616–623 (2006)
30. G.W. Fraser, J.F. Pearson, J.E. Lees, Dark noise in microchannel plate x-ray detectors. Nucl. Instrum. Methods Phys. Res. Sect. A **254**(2), 447–462 (1987)
31. N. Bloembergen, Solid state infrared quantum counters. Phys. Rev. Lett. **2**(3), 84 (1959)
32. A.F. Borghesani, C. Braggio, G. Carugno, F. Chiossi, A. Di Lieto, M. Guarise, G. Ruoso, M. Tonelli, Particle detection through the quantum counter concept in yag: Er3+. Appl. Phys. Lett. **107**(19), 193501 (2015)
33. C. Braggio, G. Carugno, F. Chiossi, A. Di Lieto, M. Guarise, P. Maddaloni, A. Ortolan, G. Ruoso, L. Santamaria, J. Tasseva et al., Axion dark matter detection by laser induced fluorescence in rare-earth doped materials. Sci. Rep. **7**(1), 15168 (2017)
34. M. Guarise, C. Braggio, R. Calabrese, G. Carugno, A. Dainelli, A. Khanbekyan, E. Luppi, E. Mariotti, M. Poggi, L. Tomassetti, Experimental setup for the growth of solid crystals of inert gases for particle detection. Rev. Sci. Instrum. **88**(11), 113303 (2017)
35. H.J. Scheel, The development of crystal growth technology, in *Crystal Growth Technology* (2003), pp. 3–14

36. J. Yoo, H. Cease, W.F. Jaskierny, D. Markley, R.B. Pahlka, D. Balakishiyeva, T. Saab, M. Filipenko, Scalability study of solid xenon. J. Instrum. **10**(04), P04009 (2015)
37. C. Braggio, R. Calabrese, G. Carugno, G. Fiscelli, M. Guarise, A. Khanbekyan, A. Noto, R. Passante, L. Rizzuto, G. Ruoso, et al., Spectroscopy of rubidium atoms in solid matrices of rare gases: experimental results and theoretical analysis. arXiv:2105.05276 (2021)
38. R. Bernabei, P. Belli, R. Cerulli, F. Montecchia, M. Amato, G. Ignesti, A. Incicchitti, D. Prosperi, C.J. Dai, H.L. He et al., Search for wimp annual modulation signature: results from dama/nai-3 and dama/nai-4 and the global combined analysis. Phys. Lett. B **480**(1–2), 23–31 (2000)
39. C. Arnaboldi, F.T. Avignone Iii, J. Beeman, M. Barucci, M. Balata, C. Brofferio, C. Bucci, S. Cebrian, R.J. Creswick, S. Capelli et al., Cuore: a cryogenic underground observatory for rare events. Nucl. Instrum. Methods Phys. Res. Sect. A **518**(3), 775–798 (2004)
40. D.V. Seletskiy, S.D. Melgaard, S. Bigotta, A. Di Lieto, M. Tonelli, M. Sheik-Bahae, Laser cooling of solids to cryogenic temperatures. Nat. Photonics **4**(3), 161–164 (2010)
41. D.V. Seletskiy, R. Epstein, M. Sheik-Bahae, Laser cooling in solids: advances and prospects. Rep. Prog. Phys. **79**(9), 096401 (2016)